NASA TECHNICAL MEMORANDUM

NASA TM X-71510

NASA TM X-71510

CLOSED CYCLE MHD POWER GENERATION EXPERIMENTS IN THE NASA LEWIS FACILITY

by Ronald J. Sovie and Lester D. Nichols
Lewis Research Center
Cleveland, Ohio

TECHNICAL PAPER proposed for presentation at
Fourteenth Symposium on Engineering Aspects of Magnetohydrodynamics
Tullahoma, Tennessee, April 8-10, 1974

CLOSED CYCLE MHD POWER GENERATION EXPERIMENTS IN THE NASA LEWIS FACILITY

Ronald J. Sovie and Lester D. Nichols
NASA Lewis Research Center
Cleveland, Ohio 44135

Abstract

Many modifications have been made in the MHD facility. These include a redesign of the MHD duct interior, addition of mixing bars, increased electrical isolation of all the high temperature components from each other and from ground, and experimentation with various cesium seed vaporization and injection techniques. With the exception of the cesium system which needs further improvement the above modifications were quite successful and resulted in improvements in generator performance. The facility was run for a total of 400 hours in the past year, with 70 hours of this operation at temperatures of 2000° K or more with hot generator walls. With the exception of replacing one cracked brick in the MHD channel no repairs were required in the high temperature loop components for the duration of these tests. Uniform Faraday and Hall voltage profiles were obtained and the Faraday open circuit voltage varied from 90 to 100 percent of the ideal u8h. The magnitudes of the measured parameters are: Faraday open circuit voltage ~70 V, total Faraday current ~20 A, Hall voltage ~250 V, power output ~300 W, and power density .036 W/cm^3.

I. Introduction

The aim of the experimental program in the Lewis closed loop facility is to evaluate the feasibility of generating MHD power with input gas temperatures of 2000 to 2100 K through the use of nonequilibrium ionization. The working fluid is a cesium seeded argon plasma. Nonequilibrium MHD power generation has been demonstrated in a shock tube facility with run times of the order of a few milliseconds[1] and a blowdown facility with run times of 10 seconds.[2]

The successful demonstration of MHD power generation in a closed loop steady state system could lead to lower weight space power generation systems and higher efficiency ground based power generation systems.[3] In the latter case the heat source for the MHD generator could be an advanced gas cooled reactor or a combustion heat exchanger.[4,5]

With the exception of the cesium seed system the closed loop facility is operated continuously with hot generator walls (~1900 K). This simulates the conditions under which a real generator must perform. In operating a facility in this manner we also obtain information on and must solve the engineering feasibility questions related to: (A) the durability of materials under long term high temperature operation, (B) maintaining the electrical insulation propertles at high temperatures and after repeated cesium injection tests, (C) design and fabrication problems, and (D) maintaining the overall loop integrity after repeated cycles of high temperature operation. In such a facility one must identify and eliminate the parameters peculiar to the facility that are adversely affecting the generator performance and then study the research problems associated with the MHD power generation. In the NASA Lewis closed cycle MHD facility the most severe problems have been the electrical isolation and seed mixing problems. The electrical isolation problems are accentuated in the steady state operation since all internal components reach high temperatures. The seed mixing problem arises since the cesium seed must be injected downstream of the electric resistance heater to avoid heater shorting problems.

At present, due to facility limitations we must operate the facility at the following conditions: gas stagnation temperature 2000 to 2100 K, gas stagnation pressure 2.2 - 2.5x10^5 N/m^2, Mach number 0.25 - 0.31, argon mass flow of 1.2 - 1.5 kg/s, and a magnetic field strength 0.1 - 1.8 T. Operation at these low Mach numbers limits the generated voltage ($V_{oc} \approx 45$ V/T) and equilibrium power level. For example, the predicted equilibrium power at B = 1 T is approximately 1 kW (power density ≈ 0.1 W/cm^3). The present goals of the program are to obtain reliable operation of the facility and exhibit nonequilibrium MHD power generation at an overall power level of a few kilowatts.

In the past year the facility was run for a total of 400 hours with 70 hours of this operation at temperatures of 2000 K or higher. This operation included 8 cycles of heating up to operating condition and cooling down. During this time no rebuilding or modification of the high temperature components including the MHD channel was required. In these tests substantial gains were made in both the facility and MHD generator performance. The present paper discusses the results obtained to date, performance improvements, and the remaining problems in the generator.

II. Facility

General Description

A detailed description of the various system components has been given previously.[6] In this paper we will give a brief description of the overall facility and then discuss the components in which changes have been made.

Figure 1 is a schematic of the closed loop facility. The gas leaving the compressor is preheated in a parallel-flow recuperative heat exchanger (preheater) before entering the graphite resistance heater. On leaving the heater through the nozzle the hot gas enters the MHD channel, expands in the diffuser, and enters the shell side of the preheater. Conventional equipment is used to further cool, dry, and filter the gas as it flows toward the compressor. Typical gas temperatures at various points in the loop and the efficiencies of various loop components are indicated in Figure 1.

The preheater is grounded. In order to obtain proper ground isolation all other components that can see the plasma are isolated from ground. The cesium is injected in the heater end bell. A series of horizontal and vertical mixing bars are placed between the nozzle exit and duct entrance.

Heater

The heater consists of an outer water cooled stainless steel shell, a lining of high density castable refractory cement, and four graphite heater elements surrounded by magnesium oxide bricks. Two major changes have been made in the heater. The heater elements are now wired in parallel and powered by 2 D.C. generators. This change has eliminated the occasional inter-element electrical breakdown previously encountered at high gas temperatures with the previous 3 phase A.C. system. The second change is that the heater elements, heater case, end bells, and piping are now all isolated from ground. This change was necessary since no matter how much care was taken to isolate the plasma and high temperature inner components from the external case the data analysis always indicated that a ground loop from the grounded preheater through the plasma to somewhere in the heater was adversely affecting the generator performance. The measured leakage resistances were acceptable before and after the tests and yet the data were ground loop limited when cesium was present. Floating the heater has alleviated this problem considerably. Except for these changes the heater has operated 1200 hours without maintenance at power levels up to 1.2 MW.

MHD Channel

A schematic representation of the channel and vaporizer arrangements is shown in Figure 2. The dimensions of the channel are length ℓ = 195 cm, height h = 19 cm, and width w = 6.35 cm. There are 28 pairs of thoriated tungsten electrodes on 2.54 cm centers located in the middle of a 91.4 cm long magnetic field region. The probes P1 and P2 serve as Hall voltage probes or may be shorted through an ammeter to measure the Hall current. The preheater tubes are grounded. The duct is electrically isolated from ground, the preheater, and the heater.

The channel construction consists of a stainless steel case lined with a high density castable refractory cement. On the channel sidewalls 2 cm thick MgO plates are bonded to the castable refractory. Layers of zirconia felt and cerafelt are located between these plates and the high density Al_2O_3 bricks that comprise the inner part of the channel. A felt covered molybdenum transition piece mates the channel with the nozzle at the channel inlet flange. This arrangement keeps the cesium from shorting the flanges together in this region.

This channel was run for 400 hours and through eight heat cycles in the past year. After this time it was necessary to replace two cracked bricks in the channel. There was no deterioration in performance from run to run. An inspection of the channel after the last run showed no evidence of cesiummigration to the flange areas or to the corners of the generator.

Cesium Injection System

Originally the cesium seed was injected in the high velocity duct entrance region. However, the data analysis showed that there was poor vapor quality and poor seed mixing along the channel width. We felt that injecting further upstream would allow more time for vaporization and mixing. The cesium is now injected in the heater end bell using a 60 cm long 2.54 cm o.d. molybdenum injection tube. In the initial tests of this concept the cesium was vaporized in a plenum located in the heater end bell and heated to the gas temperature. We have not previously injected cesium in the heater end bell becuase this arrangement introduces the risk of shorting the last heater element to the graphite lined heater end bell.

In the initial tests this seed injection system was operated in two modes. First the liquid seed is uniformly fed to the heating tube and injector, and the data are taken. Then the cesium flow control valve is closed and after a short time the cesium stored in the heating tube is blown down with high pressure argon. In the recently completed tests of this concept the blowdown tests yield about 5 seconds of uniform data at current and power levels that are double the normal data.

III. Experimental Program

Background

In references 6 and 7 it was indicated that the performance of the Lewis MHD generator was adversely affected by low resistance current leakage paths in the Hall direction. It was also shown in reference 8 that the actual vapor seed fraction in the channel, S_v, was different from that obtained from the measured liquid cesium flow rate into the vaporizer. This was caused by chugging and incomplete vaporization. Consequently, in the data analysis S_v is considered as an unknown. In order to determine S_v, the probes P1 and P2 were added to the channel (see figure 2). These probes serve as Hall voltage probes during normal performance tests. They may also be temporarily short circuited during such tests to allow the measurement of the Hall current, I_x. Simultaneous measurements of the Hall voltage, V_x, and Faraday voltages and currents give us sufficient information to determine S_v using the theory in reference 8. This theory is an extension of the results of Dzung[9] and includes the effects of finite electrode segmentation and leakage resistances in the Faraday and Hall directions.

This method was used to analyze the previously measured[10] generator performance for tests when the cesium was injected in the high velocity region of the MHD channel and the external heater case was grounded. The results indicated that the performance was limited by a Hall leakage resistance of 50 Ω and a low vapor seed fraction. It was also found[10] that there was a seed nonuniformity in the B field direction.

Analysis of the measured voltage profile indicated the 50 Ω Hall leakage resistance was caused by a ground loop that was present only during cesium injection.

In the light of these results the heater case, end bell, and all piping were isolated from ground. The cesium system was redesigned and placed in the low velocity heater end bell area. The first experimental results obtained since these changes were incorporated are given in the next section.

IV. Experimental Results

Operating Conditions

For the data presented herein the operating conditions were: gas stagnation temperature 2000 - 2030 K, stagnation pressure 2.3 - 2.5x10^5 N/m^2, argon mass flow 1.3 - 1.7 kg/s, and Mach number M = 0.25 - 0.28.

Faraday Open Circuit Voltage

The variation of the measured Faraday open circuit voltage, V_{oc}, along the channel length is shown in Figure 3. Results are presented for magnetic field strengths B of 1.02 and 1.79 T. The figure shows that the voltage profile is excellent at B = 1.02 T and that there is a slight reduction in the measured values at the ends of the generator at B = 1.79 T.

The ratio of the measured open circuit voltages at electrode pair 15 to the ideal uBh is plotted versus magnetic field strength in Figure 4. The figure illustrates the overall good behavior of the generator under open circuit conditions. The measured V_{oc} is essentially equal to the ideal for B = 0 - 1.1 T and is $\approx$ 0.9 uBh at the higher B values. These results indicate that the electrical integrity of the hot walls (~1900 K) is quite good and that there is no cesium trapping along the generator sidewalls.

Hall Voltage Measurements

The magnitude of the measured Hall voltages has improved significantly since the outer shells of the high temperature components in the generator inlet area have been isolated from ground. The variation of the measured Hall voltage with magnetic field strength is plotted in figure 5. The figure shows that in the previous tests the measured Hall voltage saturated at B $\approx$ 1 T. The present tests were not run at low B fields but the figure shows that not only is the performance at 1 T much better but the measured values increase with B up to the maximum field strength obtainable of 1.8 T. These voltages correspond to an apparent Hall parameter of approximately 1.

The figure also shows that the highest Hall voltage is obtained when the cesium system is operated in the blowdown mode rather than in normal steady operation. The same is true for the generated Faraday currents.

The variation of the Hall voltage along the channel axis is shown in Figure 6. The measured voltages are given for the generator electrode region, for probes P1 and P2, and for the cesium vaporizer (see Figure 2). The preheater tubes are 103 cm downstream from probe P2 and are grounded. Data are presented for two normal tests with Faraday load resistances R_y of 0 and 25 Ω and a test in which an external cesium supply line leak caused the vaporizer to have a resistance to ground of $\approx$ 50 Ω .

The figure shows that with the exception of electrodes 1 to 6 the generated Hall field is quite uniform along the channel length. The Hall voltage per electrode pair is larger for electrodes 1 - 6 than for the rest of the channel. This is due to an entrance end effect since the magnetic field extends beyond the ends of the generator. Corroborating evidence to this fact is that the measured currents are higher for the first few electrode pairs, and as Figure 6 shows, Hall voltage is generated in the region between probe P1 and electrode 1 for the normal tests. The figure also shows that there are no voltage drops in the region between P1 and the vaporizer. This indicates that no ground loop Hall current is flowing through the plasma and that the front end components are indeed isolated from ground.

The uniform generation of Hall voltage in the electrode area would seem to indicate that the electrode isolation is adequate. That is, there is no local failure of the electrode to electrode or electrode to ground electrical isolation. This fact alone would not necessarily mean that all is well in the generator, however. The voltage profile in the electrode region for the case when the vaporizer to ground resistance was $\approx$ 50 Ω is also quite uniform. However, in this case a ground loop current is obviously flowing through the plasma. The Hall voltage generated in the region P1 and electrode 1 has been shorted out and there is a 9 V drop between P1 and the vaporizer.

The distribution of the Faraday load voltage along the channel for the R_y = 25 data point shown in Figure 6 is given in Figure 7. The entrance effect is clearly seen in the figure. More power ($V^2/25$) is generated in the first electrode pairs. The measured power for this run (K = 0.22) was 180 watts and the equivalent power (K = 0.5) would be 270 watts.

Short Circuit Current Measurements

The variation of the short circuit current along the channel is shown in Figure 8 for normal seed injection, blowdown seed injection, and for the probes P1 and P2 shorted diagnostic test. The data were taken from the same cesium injection run. The severe effect of a low Hall leakage resistance on the performance is illustrated by the probe shorted data. Here R_x = 9 and I_x = 3 A, and comparison with the normal cesium injection data shows that the total Faraday current drops from 10 A to 3 A when the probes are shorted. The effective Hall parameter calculated using the measured current, Hall voltage, velocity, and magnetic field strength and assuming no Faraday electrode voltage drop is 6.5. The figure also shows that there is about a factor of 2 improvement in measured current with blowdown seed injection. The equivalent power ($\frac{1}{4}I_{sc}V_{oc}$) for the normal and blowdown tests are 150 and 280 watts.

Discussion of Results

The results obtained in the recent experiments have been encouraging. The measured Faraday open circuit voltages are near ideal. The variation of the measured Hall voltages with increasing B and along the channel length is much improved. The blowdown seed injection improves the measured Faraday currents. Power levels above 300 watts (.036 W/cm^3) have been obtained.

The data analysis indicates that the seed distribution across the channel width (B direction) is improved. The vapor seed rates vary from approximately .03 percent in normal injection to 0.10 percent for blowdown. The data indicate an R_x of 80 to 100 Ω but the Hall voltage profiles show no ground loop leakage or local inter-electrode

breakdown in the electrode area. A number of possible explanations for this low resistance are presently being investigated. There may be a Hall shorting loop other than a ground loop. There may be a plasma phenomenon which is indicated by the difference between the apparent and effective Hall parameters. The current density is less than 0.1 amp/cm^2 and there are some impurities of CO and H_2 so that nonequilibrium effects should not be important. It is also possible that the generator performance is not limited by an inability to hold the generated Hall voltage but that internal voltage drops in the Faraday direction actually inhibit the generation of the Faraday current and Hall voltage.[7] However, inclusion of such effects has not as yet resulted in a consistent explanation of the data obtained under the various run conditions.

Additional diagnostic tests must be made to investigate these effects and the Hall leakage resistance effects.

V. Concluding Remarks

Design changes made in the past year on the NASA Lewis closed cycle MHD facility have resulted in reliable, maintenance-free operation of the facility and have produced significant improvements in generator performance.

Isolation of the heater case and other high temperature components at the generator inlet area eliminated the ground loop Hall leakage path that had previously limited the generator performance. Installation of the cesium injection system in the heater end bell has yielded higher vapor seed fractions and better cesium mixing in the channel. Initital tests of vaporizers in the heater have led to the design of a large storage plenum and cesium injection manifold that should yield further performance improvements.

In the coming year this vaporizer will be tested and new diagnostics tests and performance tests will be run. These tests should yield further performance improvements and increase our understanding of the parameters affecting the MHD generator performance.

References

1. Zauderer, B.; and Tate, E.: Performance of a Large Scale, Nonequilibrium MHD Generator with Rare Gases. AIAA Jour., vol. 9, no. 6, June 1971, pp. 1136-1143.

2. Bertolini, E.; Gasparotto, M.; Gay, P.; Panaccione, L.; and Tamburrano, A.: Closed Cycle MHD Subsonic Power Generation Experiments at Frascati. Proceedings of the 13th Symposium on the Engineering Aspects of Magnetohydrodynamics. M. Mitchner, ed., Mississippi Univ. Press, 1973, pp. I.1.1-I.1.11.

3. Seikel, G. R.; and Nichols, L. D.: The Potential of Nuclear MHD Electric Power Systems. Paper 71-638, AIAA, June 1971.

4. Hwang, Charles C.; Smith, J. Marlin; and Seikel, G. R.: "Light Bulb" Heat Exchanger for MHD Generator Applications. Proceedings of the 13th Symposium on the Engineering Aspects of Magnetohydrodynamics. M. Mitchner, ed., Mississippi Univ. Press, 1973, pp. V.9.1-V.9.2.

5. Zauderer, B.; Marston, C. H.; Cook, C. S.; and DeDominicis, L. D.: Blowdown Test Facility for a Fossil Fueled Nonequilibrium MHD Generator. Proceedings of the 13th Symposium on the Engineering Aspects of Magnetohydrodynamics. M. Mitchner, ed., Mississippi Univ. Press, 1973, pp. IV.3.1-IV.3.6.

6. Sovie, R. J.; and Nichols, L. D.: Status of Power Generation Experiments in the NASA Lewis Closed-Cycle MHD Facility. Paper No. 72-103, AIAA, Jan. 1972.

7. Sovie, Ronald J.; and Nichols, Lester D.: Results Obtained in NASA Lewis Closed-Cycle Magnetohydrodynamic Power Generation Experiments. NASA TM X-2277, 1971.

8. Nichols, Lester D.; and Sovie, Ronald J.: Hall Current Effects in the Lewis Magnetohydrodynamic Generator. NASA TM X-2606, 1972.

9. Dzung, L. S.: Influence of Wall Conductance on the Performance of MHD Generators with Segmented Electrodes. Electricity from MHD, vol. II, IAEA, Vienna, 1966, pp. 169-176.

10. Sovie, R. J.; and Nichols, L. D.: Seed Nonuniformity and Hall Current Effects in the NASA Closed Loop MHD Generator Facility. NASA TN (to be published).

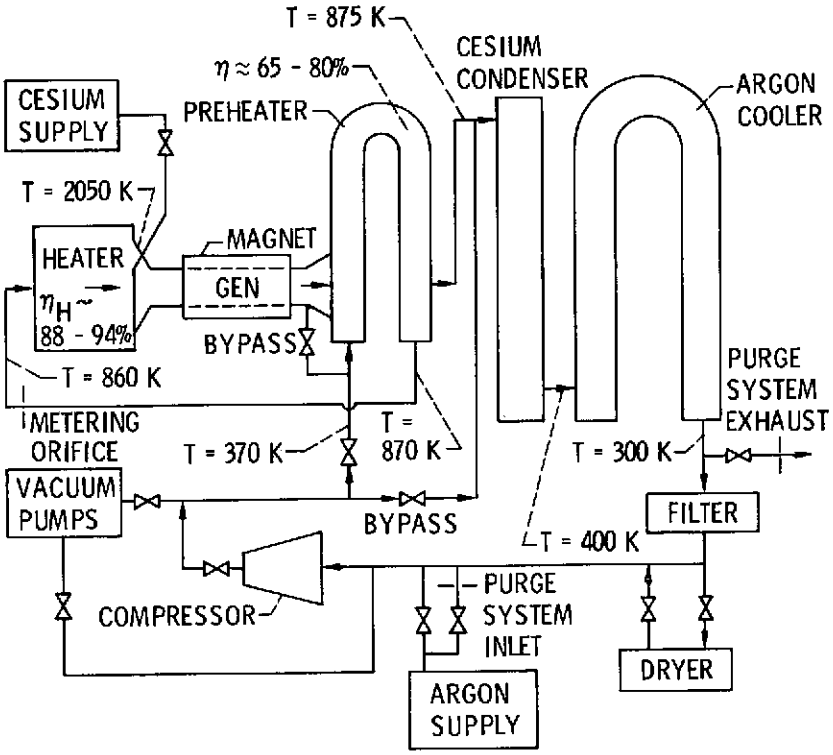

Figure 1. - Loop schematic.

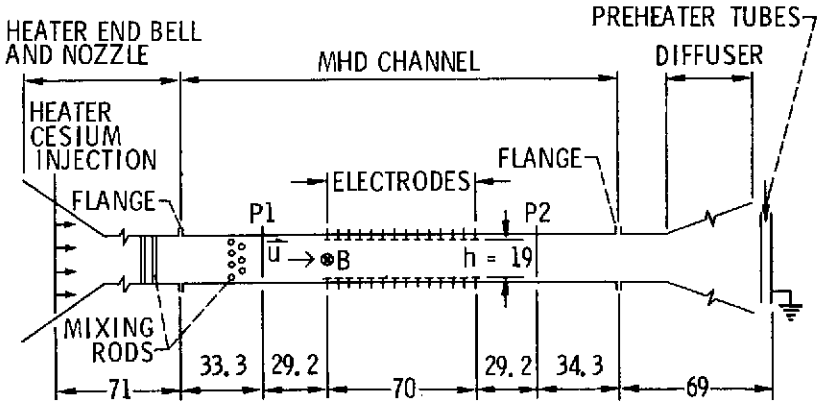

Figure 2. - Schematic representation of MHD channel and vaporizer injection point. (All dimensions are in cm.)

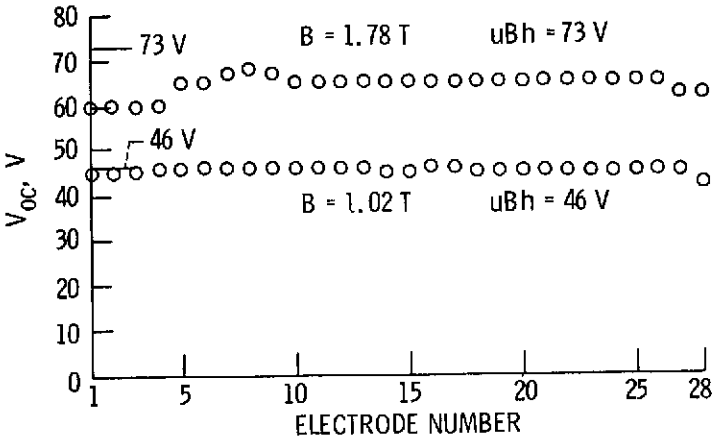

Figure 3. - Variation of the Faraday open circuit voltage along the channel length.

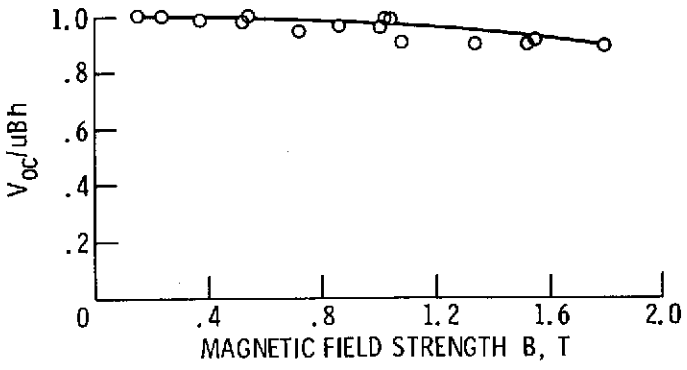

Figure 4. - Ratio of Faraday open circuit voltage, V_{OC}, to theoretical uBh versus magnetic field strength B.

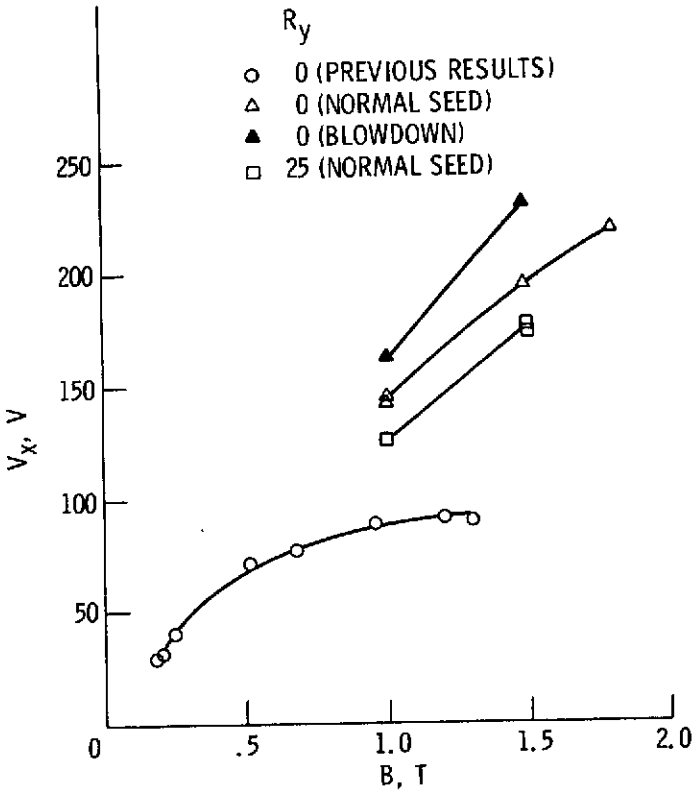

Figure 5. - Hall voltage, V_x, versus magnetic field strength B.

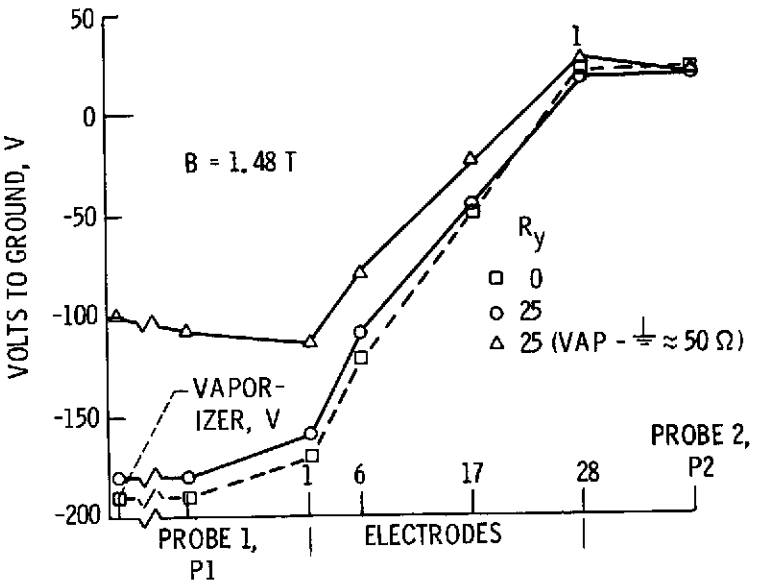

Figure 6. - Variation of the Hall voltage with respect to ground along the channel axis.

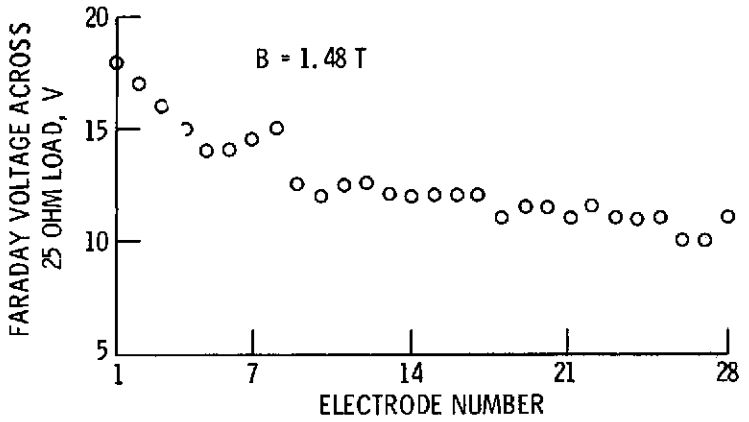

Figure 7. - Distribution of Faraday voltage along channel for $R_y = 25\ \Omega$.

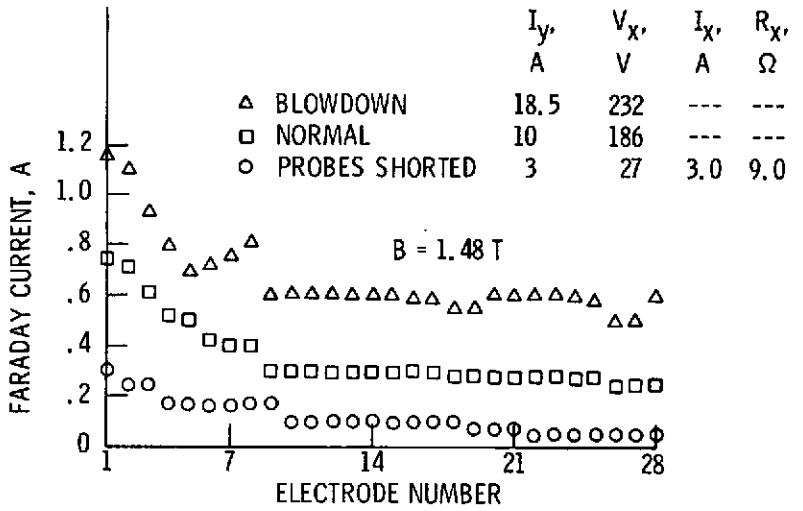

Figure 8. - Effect of shorting probes and cesium blowdown on Faraday short circuit current.